Signal Processing: Image Communication 75 (2019) 32–43

Contents lists available at ScienceDirect

Signal Processing: Image Communication

journal homepage: www.elsevier.com/locate/image

An almost complete curvature scale space representation: Euclidean case ☆

Ameni BenKhlifa *, Faouzi Ghorbel

CRISTAL Laboratory, GRIFT Research Group, Ecole Nationale des Sciences de l'Informatique (ENSI), La Manouba University, 2010, La Manouba, Tunisia

ARTICLE INFO

Keywords:
Curvature Scale Space
Almost-completeness
Curvature's levels
Shape recognition
Retrieval

ABSTRACT

Here, we intend to propose local shape curve features which are invariant under planar Euclidean transformations and independent with respect to the original curve parameterization. The present work generalizes the family of Curvature Scale Space descriptors in order to increase the shape information quantity to tend to the completeness property. For this, a more pragmatic criterion is introduced in this paper which we call the *almost completeness*. We define it as a pre-completeness for a given resolution of features. Such descriptors are formed by the curvatures on the set of curve points obtained from the antecedents of different curvature levels. This level set is fixed with a given rule. The idea of the almost completeness is to make a compromise between the cardinal of the set of curvature's levels and the optimal number of scales. The rule is submitted to an unsupervised statistical study and the scales are obtained with a spectral analysis. Experiments are conducted on several known datasets. Promising results in the sense of shape retrieval and shape recognition rates are demonstrated.

1. Introduction

Nowadays, 2D object classification field is reborn and evolves into Statistical Shape and Riemannian computing [1–5]. These fields are in vogue and they concern more complicated shapes as curved surfaces or tracking analysis like a human body tracking classification or face recognition. The 2D statistical shape seems to be a relatively simple problem with respect to surfaces representation and tracking analysis. However, there are different challenges in the sense of target performance as verifying the invariance, the completeness, the local–global well-known properties in the pattern recognition context. That is why many researchers continue to work on this direction such as [2–5].

We aim to join several ideas: the classification on shape space which is generally non-linear with the approach of invariants in order to improve the constraints required by the demanding of actual applications. Besides, this resort to the 2D object description is due to the Bigdata problem that has attacked many disciplines for many years. We mention essentially the ImageNet Large Scale Visual Recognition benchmark that collects millions of images. From 2009, researchers [6] have launched a huge challenge to create a giant dataset and to test pioneer works on the mean of shape recognition and classification [7–11].

Another field of interest is the biometry especially with the security reasons such as the war against the crime and the terrorism, the medical imaging, the computer vision, the biology, the multimedia, the remote sensing, the robotics and so on. However, reaching a good description enough with low complexity is not an easy task for many reasons. The shape is a subject to many nonlinear distortions coming from noise and occlusion or geometric transformations described by different poses. In order to overcome those problems, it requires to verify the most important properties that were mentioned in [12]:

(i) Invariance to any transformation belongs to planar Euclidean transformations group E(2).

(ii) Independence with regard to the original parameterization.

(iii) Robustness under noise and numerical approximation caused by quantification or distortion

(iv) The stability which means that if two shapes are similar to a small variation then their descriptors are similar to a small variation too.

(v) Low complexity.

(vi) Completeness which was introduced by [13] who constructed a complete and invariant set of Fourier Descriptor and defined it as a guarantee that if two shapes have the same description then they are similar.

The property of completeness is often sought because it guarantees that the descriptors carry all the information concerning the shape up to a geometric transformation. In practice, we only have access to a finite part of these descriptors. In order to illustrate this proposition, we list from the literature at least the following two categories representing most of the procedures for calculating shape attributes. The

☆ No author associated with this paper has disclosed any potential or pertinent conflicts which may be perceived to have impending conflict with this work. For full disclosure statements refer to https://doi.org/10.1016/j.image.2019.03.009.

* Corresponding author.
E-mail addresses: ameni.benkhlifa@ensi-uma.tn (A. BenKhlifa), faouzi.ghorbel@ensi.rnu.tn (F. Ghorbel).

https://doi.org/10.1016/j.image.2019.03.009
Received 9 July 2018; Received in revised form 9 December 2018; Accepted 17 March 2019
Available online 25 March 2019

first one consists in defining invariant quantities from the continuous representation of a curve. These quantities are often sequences of scalar numbers, such as the complete descriptors constructed by [13] or those obtained by Zernike of [14], or sequences of functions such as those defined from the analytical extension of the Fourier–Mellin transform by [15]. For which, it is considered only a truncation of the sequence of scalars or the sequence of functions. They are often calculated from a sampling of a continuous parameterization (1D resampling of continuous parameterization or 2D sampling of a fitted image). This does not achieve the theoretical completeness. However, it is still possible to increase the windows truncation and increase the sampling frequencies to achieve completeness only in an asymptotic manner. For example, the Fourier descriptors introduced by [16] or the seven Hu invariant moments [17] are not almost complete because, for any high window's truncation or resolution of sampling, the completeness cannot be achieved.

The second category corresponds to the case where the objects are represented in a discrete way. It is proposed to define invariant primitives from polygons or triangular meshes representations. Sometimes primitives are computed from a given procedure providing a set of key points. The reconstruction from these descriptors necessarily gives a set of finite points. Consequently, theoretical completeness, when formally possible, can only be attained by sampling with infinitely small steps tending in the best cases to the notion of re-parameterization. In this class, the example of Curvature Scale Space [18] illustrates the fact that we cannot reach the completeness asymptotically even if we increase infinitely the resolution and scale space.

It is, therefore, more realistic to consider the notion of almost completeness which can be defined as a pre-completion to a given resolution. Invariant descriptors at this resolution can be seen as the terms of a sequence converging to complete continuous descriptors.

The shape description can be classified into many categories. For the shape region description such as the Zernike moments [14], the complete complex moments [15], Chebychev discrete moments [19] etc, it suffers from the high number of features which causes low computation problem. Another problem, in that case, is the non-stability and the non-robustness to noise and numerical approximation. In the case of the affine and the projective representations, they are not robust to numerical approximation and also, they suffer from the absence of a metric on the shape space (Riemannian computing). The 3D shape one lacks especially the completeness property and it has a high complexity. Meanwhile, the 2D shape contour description under the $E(2)$ group remains one of the most simple cases. It allows us to go so far either in the description or in the classification as it was mentioned before.

Thus, we intend in this paper to propose an algorithm that ensures these above-mentioned criteria and we look forward to achieving an almost-completeness.

1.1. Related works

In the literature, the shape description technics extracted the shape features whether from the whole region or only from the boundary. Under these two families, we find two sub-classes: the global-based methods and the structural based ones. Thus, an overview of some methods of each category will be provided in the sequel.

Starting with the first class: region-based methods. They exploit the whole information that contained the pixels of the shape. These methods also will be classified into global and structural subclasses.

In the global category, they treat all the pixel information within the region. We mention the moments-based methods such as the Geometric moments proposed by [17] which have attracted a serious attention and were used in several works like [20–22]. There are also the 2D Zernike moments-based methods [14,23] and Legendre moments presented by [24] and [25]. These methods have several shortcomings such as sensitivity to local changes like occlusion or overlapping objects. In order to overcome these problems, the 2D Fourier descriptors-based methods were proposed. We mention the generic Fourier method of [26] which applied 2-D Fourier transform on polar raster sampled shape image, and the Enhanced generic Fourier in the work of [27] which derived the generic Fourier descriptor from the rotation and scale normalized shape. The multi-scale Fourier-based descriptor proposed by [28] represented the shape using its boundary and its content using the Gaussian filter in many scales. It is E(2) invariant and robust to noise. [29] introduced the analytical Fourier–Mellin transform which gave also an invariant description for the gray-level image. In the same context, we find the approach proposed by [30] which is based on a kernel descriptor that characterizes local shape. Another global-region based set of methods is the Grid-based ones. Such set applies the theory of tree-based such as the adaptive grid resolution (AGR) proposed by [31]. The ARG descriptor is acquired by applying quadtree decomposition to the bitmap representation of the shape. The advantages of the grid method are its simplicity in representation, conformance to intuition but it is sensitive to noise.

Moving to the structural family where the region was decomposed into parts. Among this category, we find the graph-based method such as the median axis transformation or skeleton. It is introduced by [32]. It consists to reduce regions to curves that follow the global shape of an object. This descriptor was used by Later by [33] used this descriptor for shape recognition. [34] used the shock graph. They decomposed the shape into a set of hierarchically organized segments of the medial axis with the monotonic flow and give a more refined partition of them.

Among the local region methods, there are these based on the calculation of gradient orientations such the pioneering work Scale-invariant feature transform (SIFT). SIFT is an approach proposed by [35,36] to detect points of interest and to extract distinctive features in order to identify them between different images. SIFT's features are invariant to rotation, translation, scale, and partially invariant to changes in affine and 3D illumination and projection. RIFT (Feature Transform invariant rotation) [37] is a rotation-invariant descriptor derived from SIFT, suitable for textured images for which the notion of principal orientation does not really make sense. Dense SIFT (DSIFT) [38] is a variant of SIFT with descriptors extracted at multiple scales. Also, the Speeded Up Robust Features (SURF) was introduced by Bay et al. in [39,40], strongly influenced by Lowe SIFTs [36], since it reflects the distribution of intensities in the vicinity of the point of interest.

The second class contains the boundary-based methods. In the global set of algorithms, we find the Fourier descriptors applied in the works of [41–43] and [12]. They extracted the global features of the contour. However other methods treat local features. We find the representation of [44] who partitioned the curve into parts at negative curvature minima which enhanced the object recognition.

A very recent work was introduced in [45], it is about a multiscale Fourier descriptor based on triangular features. Such method combines global and local features that solve the lack of local shape feature of the existing Fourier descriptors.

Triangle area representation (TAR) presented by [46] is another type of multi-scale descriptor based on the signed areas of triangles formed by boundary points at different scales. Another multiscale approach was proposed by [47]. It is called Angle Scale Descriptor and it consisted of computing the angles between points of the contour in different scales. [48] proposed to characterize the contour with two intrinsic properties: its length and the curvature variations and use them for registration and matching. Their method is called Curve Edit. There is also the method of [49] which consists of an algorithm called the Shape Context. At each reference point of the contour, they captured the distribution of the remain points. For two similar contours, the corresponding points had similar shape contexts. This correspondence gives an optimal registration. [50] suggested a new distance called the Inner-Distance. It is defined as the length of the shortest path between feature points. This distance can replace the Euclidean distance for complex shapes. It was combined with several methods such as the Shape context. [51] developed a mechanism to generate a coarse segment matching between different instances of an object and they employed a natural correspondence of skeletal branches to sequential segments along the contour. [52] proposed another method called contour flexibility which represents the deformable potential at each point of the contour.

In the part based sub-class, a work was introduced by [53] based on the segmentation of the silhouette. [54] proposed the use of the curvature zero-crossing points from a smoothed contour to get the parts, called tokens. The orientations and the maximum curvatures of the obtained parts are taken into account to represent shapes and matching. In the work of [55] gave a representation for shape-based recognition based on the extraction of the perceptually relevant fragments. According to this approach, each shape is transformed into a symbolic representation, using a predefined dictionary for the contour fragments, which is mapped to an invariant high-dimensional space that is used for recognition. [56] proposed to distribute the parts of a contour under polar coordinates. Their representation is called Contour Points Distribution Histogram. It is simple, and the Earth Mover's Distance used is flexible which allow a low complexity. [57] presented a Shape Saliences Descriptor (SSD). The salience points are the higher curvature ones. They were represented using the relative angular position and the multiscale analyzed curvature values. There is also the work of [58] which is a part-based approach for contour description called Curve Normalization. They represented the shape boundary by an ordered sequence of parts. Then, they associated each part with the cubic polynomial curve using the Least Squared method. Another well-known local description called the Curvature Scale Space (CSS) was introduced by [18]. It is obtained by the extraction of the zero-crossing points of the smoothed contour parameterizations by a succession of Gaussian functions in different scales. [59] proposed to extract the extrema of the same set of functions used by [18]. Several authors such as [60] have been developed other variants of such descriptors and many others applied them massively in retrieval, shape classification and so on because of their good behavior (as the E(2) Invariance, the robustness, and their compactness). This efficient description has been enriched in our past work [61] (GCSS) by considering an invariant feature on curve points having a given level set of curvatures.

1.2. Our approach

In the present paper, we intend to propose a novel 2D contour representation. Our description is E(2) invariant, robust to noise, almost-complete which we defined it as a pre-completeness for a given resolution and independent to the original parameterization. In our previous work [61] we have introduced a generalization of the well-known curvature scale space family [18,59] by enriching the shape information quantity through geometric spaces at different scales. The idea of the construction of these descriptors is to compute the curvature on a different set of curve points. They come from the curvature's levels that are superior to a given threshold. This representation depends on these parameters: threshold and scales which were fixed empirically. Here, we propose to adjust them according to criteria in order to attain the almost-completeness property. A statistical one for the choice of curvature's threshold. Expectation Maximization algorithm followed by the Bayesian classifier is applied to finding it. The second criterion comes from a spectral analysis. It is operated in order to fix the appropriate scales. The output of this process consists of a set of key points which is different from a contour to another. Therefore, a discrete normalization step is performed. The final descriptors are composed by the curvature values of these normalized key points.

The main contributions of this paper are the following:

- The computation of the threshold relative to curvature's levels.
- The determination of the optimal scales by a spectral analysis approach.
- The introduction of the almost completeness notion in order to give another comparative criterion between descriptors.

We test the performance of the proposed description on several datasets. Results are promising especially with the low complexity and the other interesting properties of the introduced representation.

This paper is organized as follows. In the second section, a detailed description of our proposed algorithm will be given. In the third section, the used similarity metric that corresponds to the Dynamic Time Warping will be exposed. In the fourth section, we will evaluate and discuss the results of the application of our approach using several datasets and we will give a comparative study with the state of the art. Finally, some conclusions will be exposed.

2. The proposed description

The curve Γ is assumed to be closed and injective. It is well-known that this kind of curves can be represented by a periodic parameterization defined as the function $C(\zeta)$:

$$\begin{aligned} C &: [0,1] \to \mathbb{R}^2 \\ \zeta &\mapsto [x(\zeta), y(\zeta)]^t \end{aligned} \tag{1}$$

Where $x(\zeta)$ and $y(\zeta)$ are the coordinates of a point curve at the time ζ. It is important to note that the parameterization of the curve is not unique because it depends upon the starting point and the speed we go over the curve. To get rid of this problem, the arc length reparameterization is generally chosen as a solution since it is invariant under Euclidean transformations.

$$s(\zeta) = 1/L \int \sqrt{x_\zeta(u)^2 + y_\zeta(u)^2}du, \qquad \zeta \in [0,1] \tag{2}$$

Where L denotes the total length of the contour Γ. This step is important because it simplifies the curvature function's computation.

2.1. Recall of generalized curvature scale space

The construction of this representation implies three main steps. They will be repeated for a given set of scales chosen empirically:

1. The convolution of the contour by a given Gaussian function and the calculation of the curvature variation of the smoothed contour.
2. The extrema's extraction from the curvature variation and thresholding application.
3. The extraction of the points having the same curvature values as the remaining extrema

The steps of GCSS will be detailed in the following paragraphs also they are illustrated in Fig. 1 for a given scale.

2.1.1. The computation of the curvature scale space

The curvature scale space (CSS) which was introduced firstly by [18] represents the shape boundary Γ at multiple scales. It consists of the extraction of the curvature zero-crossing points in a given set of scales. Let denote by C_σ the smoothed contour parameterized by the normalized arc length for a fixed scale σ:

$$C_\sigma : [0,1] \to \mathbb{R}^2 \tag{3}$$

$s \mapsto [x(s,\sigma), y(s,\sigma)]^t$

Where:

$$\begin{cases} x(s,\sigma) = x(s) \bigotimes g(s,\sigma) \\ y(s,\sigma) = y(s) \bigotimes g(s,\sigma) \end{cases} \tag{4}$$

$g(s,\sigma)$ is a Gaussian function and $\bigotimes$ is the convolution product. The expression of the smoothed contour curvature $\kappa(s,\sigma)$ according to a normalized arc length is given as follows:

$$\kappa(s,\sigma) = \frac{x_s(s,\sigma)y_{ss}(s,\sigma) - y_s(s,\sigma)x_{ss}(s,\sigma)}{(x_s^2(s,\sigma) + y_s^2(s,\sigma))^{3/2}} \tag{5}$$

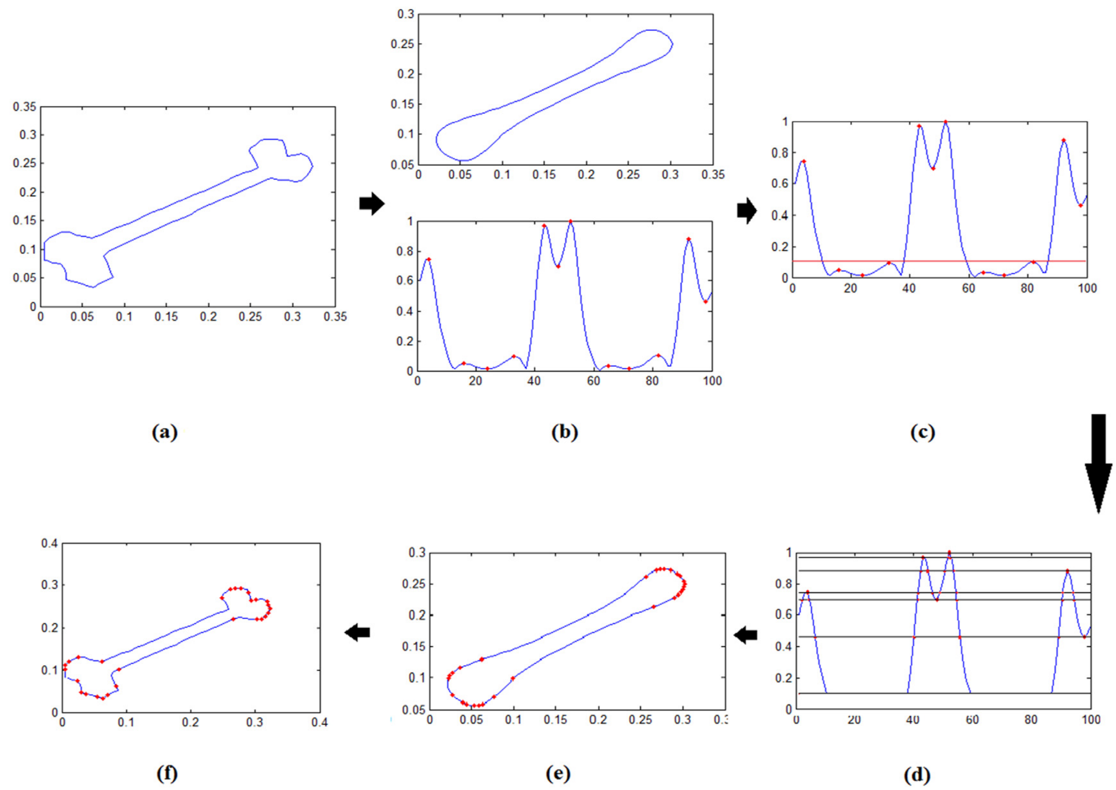

Fig. 1. The steps of GCSS. (a) the original contour (b) CSS image and its curvature variation in a given σ (c) Thresholding (d) the key points detection (e) the key points on the smoothed shape contour (f) the key points on the original contour.

Where $x_s(s,\sigma)$, $y_s(s,\sigma)$, $x_{ss}(s,\sigma)$ and $y_{ss}(s,\sigma)$ represent respectively the first and the second derivatives of $x(s,\sigma)$ and $y(s,\sigma)$ and they are given by:

$$\begin{cases} x_s(s,\sigma) = x(s) \bigotimes g_s(s,\sigma) & x_{ss}(s,\sigma) = x(s) \bigotimes g_{ss}(s,\sigma) \\ y_s(s,\sigma) = y(s) \bigotimes g_s(s,\sigma) & y_{ss}(s,\sigma) = y(s) \bigotimes g_{ss}(s,\sigma) \end{cases} \tag{6}$$

2.1.2. The extrema extraction and thresholding

Once the curvature function of the smoothed contour is obtained, the next step corresponds to the extrema extraction and the thresholding. CSS provides the curvature zero-crossing points. Although its robustness to scale, noise and orientation, it has some inconveniences. We can mention its inefficiency in cases of deep and shallow concavities. Hence, Extreme Curvature Scale Space (ECSS) of [59] was provided as a solution. It tracked the curvature extreme points. The set of points, which are formed by the inflection ones of a smoothed curve at a scale σ, is denoted by ℓ_σ.

By increasing σ, C_σ becomes smoother and the number of extrema decreases more and more.

However, there is many local extrema that have low absolute curvature variations. Therefore, we performed a thresholding in order to eliminate them. To introduce only one threshold τ, we consider absolute curvature variations. The extrema higher than τ are kept in $\ell_\sigma(\tau)$ which can be formulated as follow:

$$\ell_\sigma(\tau) = \{\kappa \in \ell_\sigma \quad ; |\kappa| > \tau\} \tag{7}$$

This step is important because we are looking for local extrema which have significant curvature variations in the mean of shape information. In our past work, the threshold was retained empirically. In Section 2.2, we propose Bayesian decision for the determination of τ.

2.1.3. The key points detection

The next step consists of seeking the points of the contour having the same curvature values as the set $\ell_\sigma(\tau)$. For that purpose, we extract the reciprocal image of the singleton $\kappa_\sigma^{-1}(\{\ell_\sigma(\tau)\})$ described in Eq. (8). This step is done because the curvature function is not bijective.

$$\kappa_\sigma^{-1}(\{\ell_\sigma(\tau)\}) = \{s \in [0,1] \quad / \kappa_\sigma(s) \in \ell_\sigma(\tau)\} \tag{8}$$

The selected points at each scale σ are stored in a $F_c(\sigma)$. They can be described as follows:

$$F_c(\sigma) = \{C(s,\sigma) \quad / s \in \kappa_\sigma^{-1}\{\ell_\sigma(\tau)\}\} \tag{9}$$

In order to determinate the optimal scales Σ in the mean of the shape information. They are identified with respect to Shannon rule. Thus, for each $\sigma \in \Sigma$ where $\Sigma = \sigma_1..\sigma_n$ (n the number of the chosen scales) we obtain the following F_c.

$$F_c = \bigcup_{\sigma \in \Sigma} F_c(\sigma) \tag{10}$$

ECSS, as well as CSS, are not complete. We aim to make this representation rich in order to ensure also this property. The smoothed contour here is not only described by its extrema. So, we enhance this representation by adding more points in high curvature and eliminate those in monotonous zones. Fig. 2 shows an example of a contour represented by ECSS then by GCSS and the difference between them. It is obvious that GCSS focus on the regions with high curvature variations.

2.2. Statistical study on the threshold

Before we proceed EGCSS computing for each contour apart, we must fix the good threshold to apply. It will lead to a better selection of the extrema which represents a unidimensional clustering problem. The application of Expectation Maximization (EM) algorithm in the present context allows us to decide with a Bayesian rule which minimizes the probability of error. Therefore, we consider the set of extrema curvature values for the whole dataset in several scales. We assume that they are the observations of a Gaussian Mixture of K classes. We identify the

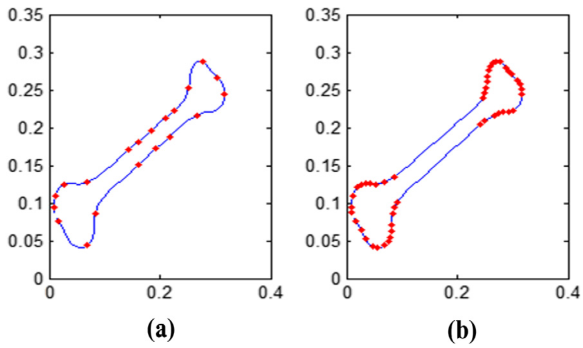

Fig. 2. Two smoothed contours of the same query with $\sigma = 2$ (a) The extreme curvature scale space representation (b) Generalized curvature scale space representation.

mixture by applying an algorithm from Expectation Maximization (EM) family. The selected threshold corresponds to the maximum value of the intersection set of the conditional density of probability, describing the class K_0 of the lowest curvature values, and the rest of the mixture which can be formulated as follows:

$$\tau = max\{\pi_{K_0} f_{K_0} = \sum_{K \neq K_0} \pi_K f_K\} \tag{11}$$

Fig. 3 illustrates the process of threshold computing. We notice that if a contour has many deformations, the class K_0 becomes very small and the threshold approaches 0. So, the points of the curve, which has a finite resolution, will be reached by the descriptors. This fact justifies the almost completeness property of our description.

2.3. Optimal scales determination

For two different shapes, we always end up with ellipses in the latest values of σ of the Curvature Scale Space description. We propose to find the highest value σ_{max} that keeps the outline of the original contour (before smoothing). It is estimated with a spectral study. We proceed the 2D Fourier Transform of the bidimensional components of the smoothed contour points $x_\sigma(s)$ and $y_\sigma(s)$. We identify the information zone and the noise one by applying Shannon rule in scale space until the high frequencies become null for each component apart. Consequently, we obtain σ_1 and σ_2 from $x_\sigma(s)$ and $y_\sigma(s)$ respectively (Fig. 4) and $\sigma_{max} = max(\sigma_1, \sigma_2)$, is the limit scale.

We opt to consider a set of scales that are formed of fractions of σ_{max}. The number of fractions retained is dictated by the cardinal of the descriptors fixed in advance.

It is important to mention that we are not learning to deliberately choose scales because we are aiming for points shape containing information for each contour apart.

2.4. The discrete normalization

Let $N = card(\digamma_c)$ the number of the obtained unordered key points. We sort them according to their appearance on the curve. We denote the wished number of key points by N_w. In order to obtain N_w interest points from the total N, we apply the following steps:

1. The cumulative distance computing.
2. The regular resampling.

2.4.1. The cumulative distance computing

The first step of our process is the cumulative distance calculating between the starting point P_1 and P_i where i the ith point of Γ. Therefore, a finite function from $1..N$ to an interval $[0, a]$ from $\mathbb{R}$ is defined. So, we consider $S(P_i)$ defined in (12):

$$S(P_i) = \int_{\widehat{P_1, P_i}} \|C'(s)\| ds \tag{12}$$

2.4.2. The regular resampling

After obtaining the function of cumulative distances $S(P)$, we move on to the resampling procedure. We resample the vector $[P_1..P_N]$ into $[P_1^*..P_{N_w}^*]$. We compute $S(P_i^*)$ and we search the nearest points $S(P_j)$.

$$\underset{j}{\text{argmin}} \|S(P_i^*) - S(P_j)\| \tag{13}$$

Fig. 5 gives an illustration of the proposed normalization procedure from $N = 28$ to $N_w = 10$.

2.5. Computation of the curvature values of the points of interest

After normalization, we obtain a set of points coming from the found key points. This set describes well the contour in the high variation zones and it is relative invariant. Meanwhile, we seek an absolute invariant representation, therefore, we choose to compute the curvature variation of our points convoluted by a Gaussian function in σ_{max} which described the following $\digamma$:

$$\digamma = \kappa_{\sigma_{max}}(\widehat{\digamma_c^*}) \tag{14}$$

It is important to mention that $\digamma$ can be changed as needed by calculating an other intrinsic property (Such as the angle function relative to the tangent vector on the starting point). The details of the various stages of the proposed description are depicted in Fig. 6.

The rule of the choice of the curvature's levels could be modified according to the type of shapes in the dataset. In an extreme case, if the contour is very smooth, σ_{max} is near to 0 and the obtained number of key points is always lower than N_w. Thus, we change the rule by adding levels such as the mean values between the extrema and so on.

2.6. Properties of EGCSS

Many properties are insured by our representation such as the almost completeness, the invariance to E(2) transformations, the stability, and the robustness to numerical approximation.

2.6.1. The almost completeness

Theoretically, complete descriptors carry all the information concerning the shape up to a geometric transformation. However, in practice, it is not reachable. So, we introduce the almost completeness notion. It can be defined as a pre-completeness to a given resolution. Invariant descriptors at this resolution can be seen as the terms of a sequence converging to complete continuous descriptors.

Thus, we aim here to reach this important property by increasing the number of key points. The applied rule in order to ensure the completeness was the use of the extrema. However, we can change the rule and increase the number of key points whether by choosing multiple scales or by dividing the curvature function into equidistant levels. As much as the number of levels is increased, the whole contour points could be reached and of course, the almost completeness property is insured (see the Appendix).

2.6.2. The invariance to E(2)

Enhanced Generalized Curvature Scale Space descriptor is based on the computation of the curvature of the smoothed contour in given scales. As the curvature behavior is the same whatever is the transformation applied to the contour: rotation, translation or scale, the obtained set of points of Γ and $g(\Gamma)$ is the same where g is an E(2) transformation.

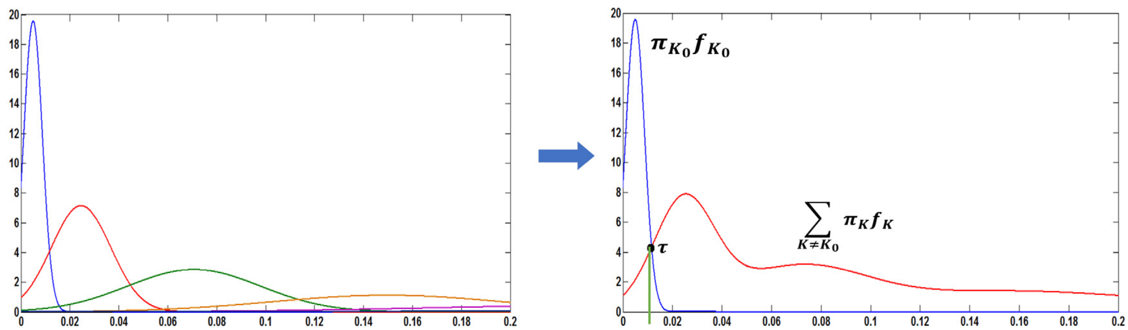

Fig. 3. Threshold computing (left) K densities of probabilities of K classes (right) Identification of the first class and the rest of the mixture and the threshold determination.

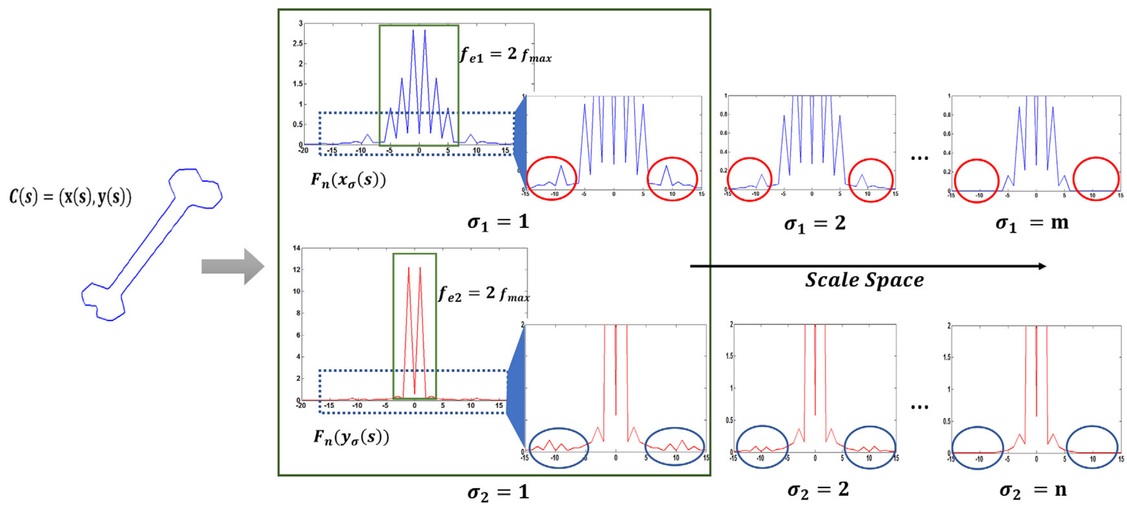

Fig. 4. The process of the limit scale determination.

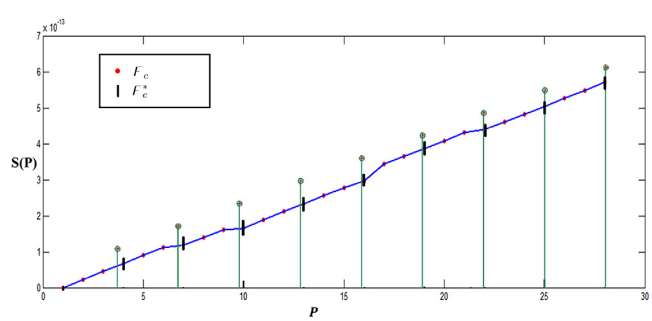

Fig. 5. A normalization example from $N = 28$ to $N_w = 10$.

2.6.3. The robustness to noise

Here, the stability is assured by three reasons:

- Enhanced Generalized Curvature Scale Space is based on the convolution of the contour with Gaussian functions in different scales. The smoothness process of the contour makes our descriptor more stable to local deformations.
- The threshold allows to eliminate the low curvature variation extrema that are considered as noise.
- The number of points chosen is high enough to describe the curve.

Moreover, in order to evaluate the stability of our descriptors, we add Gaussian noise to a given contour and see its impact on the output vector. We also test the robustness of our description in the next Section 4.6 by perturbing a whole dataset (Kimia99 elaborated by [33]) and computing its retrieval rates. As we can observe in Fig. 7, we superimpose the variations of two set of features: the first of an original contour and the second of the perturbed contour by Gaussian noise with $\sigma = 0.4$. We remark that our descriptors are stable and robust to noise.

3. Similarity metric

In order to compare between 2D contour descriptors, we use the Dynamic Time Warping distance introduced by [62] as a similarity metric. The proposed representation gives a pseudo time series and the DTW ensures the invariance relatively to the starting point as mentioned in [63]. Let suppose that we have two contours A and B. They are represented by two signatures $\mathcal{F}(A) = \{\mathcal{F}(a_1), \mathcal{F}(a_2)..\mathcal{F}(a_{N_w})\}$ and $\mathcal{F}(B) = \{\mathcal{F}(b_1), \mathcal{F}(b_2)..\mathcal{F}(b_{N_w})\}$ respectively for A and B of length N_w both. The distance between these two series is the path that minimizes the

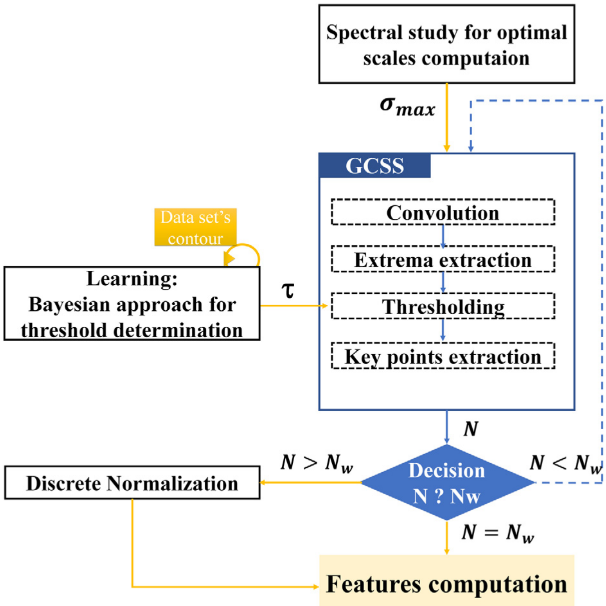

Fig. 6. The blockdiagram of EGCSS.

cumulative distance between them $D(\mathcal{F}(a_i), \mathcal{F}(b_i))$.

$$D(\mathcal{F}(a_i), \mathcal{F}(b_j)) = min \begin{cases} D(\mathcal{F}(a_i), \mathcal{F}(b_{j-1})) \\ D(\mathcal{F}(a_{i-1}), \mathcal{F}(b_j)) \\ D(\mathcal{F}(a_{i-1}), \mathcal{F}(b_{j-1})) \end{cases} + D(\mathcal{F}(a_i), \mathcal{F}(b_j)) \tag{15}$$

4. Experiments and results

The performance of EGCSS is tested on five datasets and evaluated in terms of shape recognition, shape retrieval efficiency and precision–recall curve. The experiments on these datasets are carried on: HMM GPD [64,65], MPEG7 CE Shape-1 Part-B [66], Swedish Leaf [67], ETH-80 [68], kimia99 and kimia216 [33].

4.1. MPEG7 CE Shape-1 Part-B

The well-known MPEG7 CE Shape-1 Part-B dataset [66] is composed of 1400 elements that are grouped in 70 classes. Each class contains 20 images (Fig. 8).

The obtained threshold for this dataset is $\tau = 10^{-2}$. In order to fix the adequate number of points of interest, we applied our approach for the task of recognition rate using the one nearest neighbor(1NN) algorithm on the MPEG7 dataset. Fig. 9 illustrates the performance of EGCSS on this database for different N_w. It is obvious that $N_w = 50$ gives the best recognition rate which is 93.24%. It is clear that we obtain good results with a low number of key points. This fact decreases the complexity of the matching step.

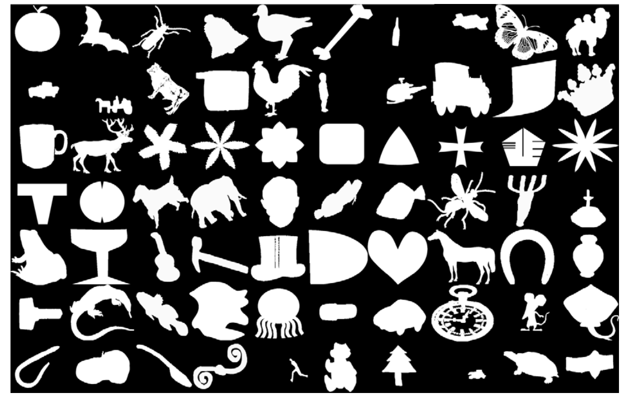

Fig. 8. Samples from MPEG7 Set B dataset.

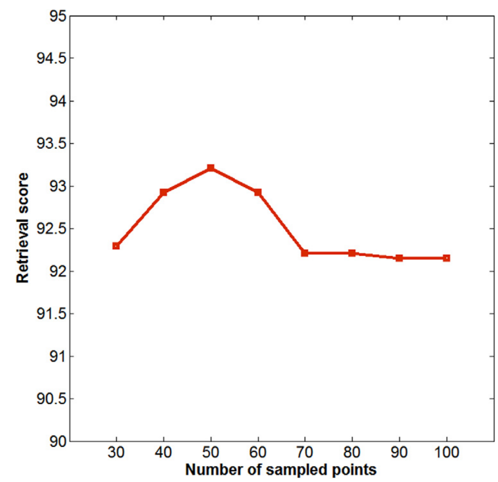

Fig. 9. Dependency of the retrieval rates and the number of points.

The performance of the proposed descriptors is compared with other approaches in the literature. The retrieval rates are measured with the Bull's eyes algorithm. Each shape is considered as a query and we count how many objects within the 40 most similar objects belong to the class of the query. Table 1 lists the Bull's eye scores of some algorithms. We remark that our algorithm gives a competitive score comparing to the Contour Points Distribution Histogram (CPDH) [56], Shape Contexts [49], Visual Parts [69], CSS [18], Visual parts [69], SSD [51], ASD [47], Curve normalization [58]. However, the score is not very important due to the high intra-class variation and the presence of symmetrical objects.

In order to simulate the occlusion, [70] generated 100 different combined shapes by merging two randomly chosen ones as shown in Fig. 10.

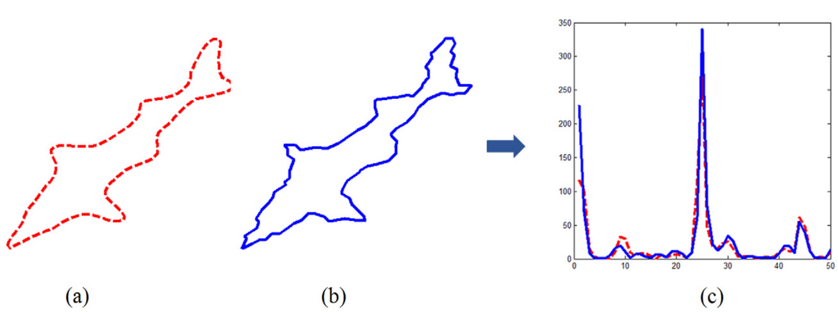

Fig. 7. The robustness to noise (a) Original contour (b) Perturbed contour (c) The descriptions of the two contours.

Table 1
Bull's eye MPEG7 setB.

Contour flexibility	89.31%
IDSC	85.40%
Is-match	84.97%
Skeletal context	79.92%
Ours	78.84%
CPDH	76.56%
SC	76.51%
Visual parts	76.45%
CSS	75.44%
ASD	70.51%
SSD	61.00%
Curve normalization	50.76%

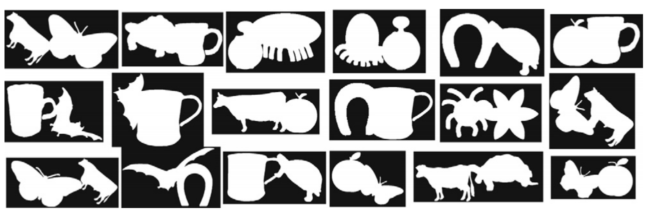

Fig. 10. Examples from Merged Mpeg7 dataset [70].

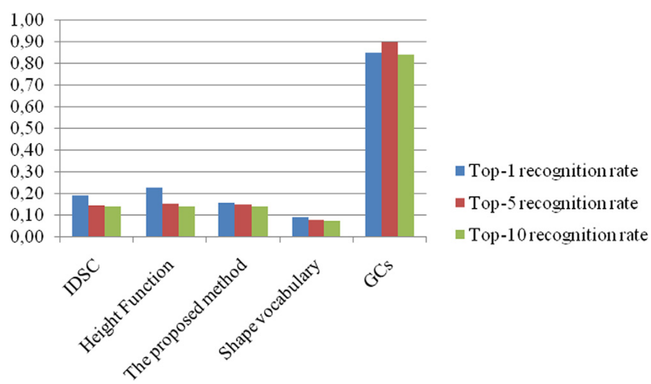

Fig. 11. Retrieval results on Merged Mpeg7 dataset.

We compare the Top-1, Top-5 and Top-10 recognition rates for 100 combined shapes on the MPEG-7 dataset with IDSC [50], Height functions [71], Shape vocabulary [72], and GCs [70] in Fig. 11. This last method outperforms the other ones because of its global criteria. Here also we can understand that a global information is needed to enhance the recognition in the case of occluded shapes. However, our method (as well as IDSC, Height functions and Shape vocabulary) handles local criteria. That is why it would be necessary to add global criteria to our descriptor to overcome the limitation in case of occlusion.

4.2. Swedish leaf dataset

In order to evaluate our algorithm on real images, we use the Swedish leaf [67] dataset. It contains 1125 unsegmented images from 15 different classes of leaves (75 objects per class) shown in Fig. 12. It is important to notice that such dataset contains many indistinguishable species. In the experiments, we randomly select 25 training images from each class and classify the remaining images using the 1NN algorithm. Table 2 lists the results of our recognition rate to other methods from the state of the art. We note that our results are average due to the similarity of the shapes as abovementioned. To improve our results, we propose to introduce a global information to overcome such limitations. The threshold for these experiments is $\tau = 0.001$ and the chosen number of key points is $N_w = 100$.

Fig. 12. One example per class for the Swedish leaf dataset [67].

Table 2
Recognition rates for Swedish leaf dataset [67].

Algorithm	Score %
Triangle centroid area FD [73]	70.26
Soderkvist [67]	82.4
SC+DP [49]	88.12
The proposed method	88.70
IDSC+DP [50]	94.13
Shape tree [74]	96.28
Multiscale FD [45]	97.6

Fig. 13. ETH-80 dataset.

4.3. ETH-80

The ETH-80 [68] dataset contains 3280 objects. They are grouped in eight categories. Each category has 10 objects and for each one of them there are 41 images from different poses(8 × 10x41=3280) (Fig. 13). The threshold of this dataset is $\tau = 0.014$ and the number of points of interest is $N_w = 50$.

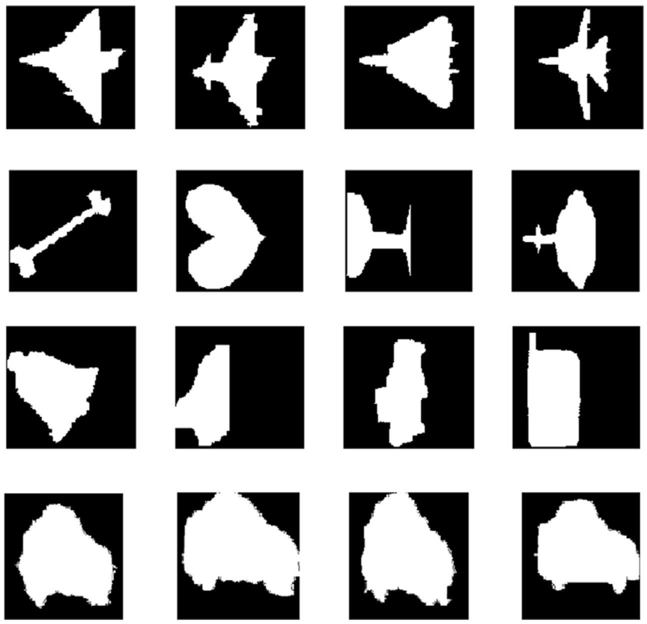

Fig. 14. Samples from HMM-GPD dataset.

Table 3
Recognition rates for ETH-80 [68].

Algorithm	Score %
IDSC	88.11
EGCSS	87.5
SC	86.40

For the recognition, each object is compared to the 79 other objects. It is considered successful if the tested one was attributed to the right category.

Table 3 lists the recognition rates of the Enhanced Generalized Curvature Scale Space and other methods from the state of the arts. The reached recognition rate is competitive and encouraging.

4.4. HMM GPD

The HMM GPD is composed of four sub datasets as shows the following Table 4: bicego-data [65], plane-data, mpeg-data and car-data [64]. We form a dataset using the four sub datasets (bicego, plane, car and mpeg) by picking up the 20 first elements of each class. Fig. 14 gives some samples of HMM-GPD dataset.

We obtain here as a threshold $\tau = 0.01$. The chosen number of points of interest is $N_w = 50$.

Table 5 lists the retrieval results of our description EGCSS on HMM GPD dataset using 1NN algorithm (For the recognition, each object is compared to all the shapes in the dataset using the Dynamic Time warping algorithm and matched to the closest one). We reach very high score for Mpeg (100%) and Plane (98.57%) datasets. Although the Car sub-dataset contains bad quality contours, EGCSS outperforms CSS of [18] and reaches 77.50%. This demonstrates well the robustness of EGCSS to numerical approximation. This robustness is due to the use of the multiscale approach in the construction of the proposed representation.

Table 4
HMM GPD sub-datasets.

Sub-dataset	Objects	Classes
Bicego	140	7
Plane	210	7
Car	120	4
Mpeg	120	6
HMM	480	24

Table 5
Retrieval results on HMM dataset using 1NN algorithm for: EGCSS and CSS [18].

	Rate EGCSS (%)	Rate CSS (%)
Bicego	94.50	90.00
Plane	98.57	79.52
Car	75.50	55.00
Mpeg	100	95.83
HMM	85.00	75.62

4.5. KIMIA 216

Kimia 216 is a dataset elaborated by Sebastian et al. [33]. It contains 216 shapes grouped in 18 classes. Fig. 15 shows one sample of each class.

For Kimia 216 dataset, we find $\tau = 0.011$ and we fix $N_w = 50$. In order to study the retrieval performance of our descriptors on this dataset, each shape of the 216 shapes was considered as a query. Then, the shapes within the same class of the query in the 12 nearest shapes are computed. Fig. 16 shows well that our algorithm reaches 100% for five classes (Bone, Glass, Children, Face, and Fountain) and high scores for the next seven classes (higher than 90%). The achieved retrieval rate is 88.22% and it is higher than the rate reached by [58] which is 73.95%. Using 1NN algorithm, we achieve 94.44%. These results demonstrate well the effectiveness of our proposed algorithm.

4.6. KIMIA 99

Kimia 99 is also created by [33]. It consists of 9 classes composed by 11 objects as shows Fig. 17. This dataset contains many objects that have missing parts, occlusion or deformations.

For the experiments, the used threshold is $\tau = 0.0089$ and the number of points of interest is $N_w = 50$.

Fig. 15. Samples from kimia 216 dataset.

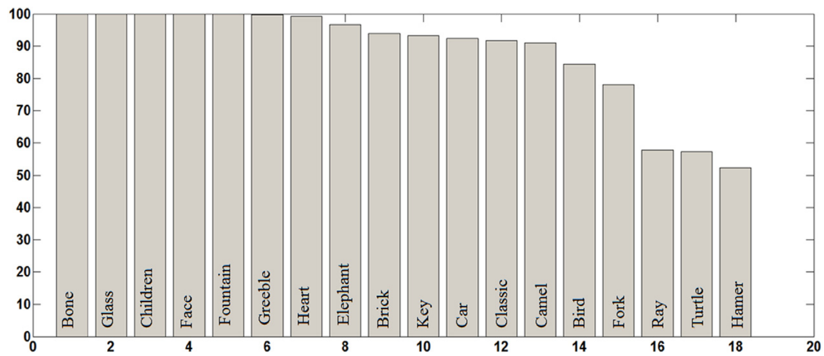

Fig. 16. Retrieval rates per class obtained by the proposed algorithm for the Kimia-216 database.

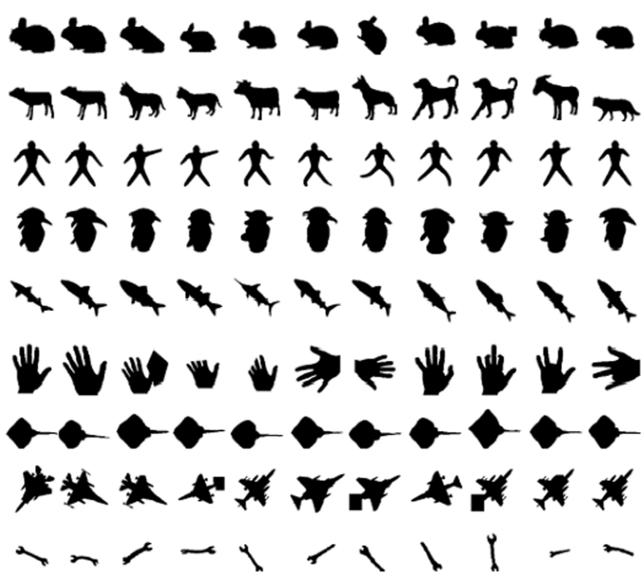

Fig. 17. Kimia 99 shapes.

Table 6
Kimia 99 retrieval rates.

SC	97	91	88	85	84	77	75	66	56	37
Proposed method	99	98	94	92	88	86	81	78	75	71
HC	96	84	78	77	78	65	68	58	66	48
Curve normalization	97	86	87	75	76	70	55	53	46	44
IDSC	99	99	99	98	98	97	97	98	94	79
Path similarity	99	99	98	98	98	97	96	94	93	82
Two strategies	99	99	99	98	99	99	99	97	96	84

All the 99 shapes have been considered as query shapes. The retrieval result is the number of the correct matches in the 10 closest shapes computed for each query. Table 6 lists the retrieval results of EGCSS and some methods of the state of the art (SC [49], HC [75], Curve normalization [58], IDSC [50], Path similarity [76], Two strategies [77]). It is obvious that our algorithm gives competitive results comparing to other methods.

In order to evaluate the performance of our algorithm under noisy conditions, we apply Gaussian noise to the outer contour of all the shapes in kimia99. Fig. 18 shows a contour with increasing Gaussian noise (σ from 0.2 to 0.8). Table 7 depicts well that although the shapes get noisier, the retrieval results do not decrease. It is proof of the stability of our representation and its robustness to Gaussian noise.

Table 7
Kimia 99 retrieval rates under noise.

$\sigma = 0$	99	98	94	92	88	86	81	78	75	71
$\sigma = 0.2$	99	98	93	89	86	84	80	78	75	72
$\sigma = 0.4$	99	97	92	90	86	85	80	78	74	71
$\sigma = 0.6$	99	98	92	89	85	83	80	77	74	70
$\sigma = 0.8$	99	98	92	90	86	84	80	76	74	70

5. Conclusion

In this paper, we proposed a plane curve description. It is local, E(2) invariant, robust to noise and independent to the original parameterization. In our previous work [61] we have introduced a generalization of the well-know curvature scale space family [18,59] we enrich the shape information quantity through geometric spaces while optimizing the number of scales. These descriptors are formed by the curvatures on a given set of curve points. Here, we have adjusted the threshold and the scales. Expectation Maximization algorithm followed by Bayesian classifier was applied to finding the threshold. For the optimization on the scale space, a curve spectral analysis has been used. A discrete normalization has been performed on the descriptors in order to be able to apply any classifier. The performance of the representation was tested on different datasets (MPEG7 CE Shape-1 Part-B (4.1), Swedish Leaf (4.2), ETH-80 (4.3), HMM-GPD (4.4), KIMIA 216 (4.5) and KIMIA 99 (4.6)). The obtained results show that the proposed method provides an improvement relative to its family of descriptors because of its performance in the sense of precision and complexity. A very important property of this representation that was proven is its robustness to noise. It is easy to implement and it has the local characteristic that is in many resolutions at the same time. Also, it is always possible to change the rule of the descriptors construction. This fact gives us other possibilities to improve results.

In future work, there are many ways to explore. We can extend it to the affine case since it is more realistic for the computer vision. An interesting and up to date perspective consists of 3D curves representation especially for the gait analysis of skeletons. We aim also to immigrate to the 3D shape space and study the property of almost completeness in the 3D case. Also, we are working on a Deep Generalized Curvature Scale Space in order to test on the ImageNet dataset [6].

Acknowledgments

This research was realized in Cristal Lab-Grift research group in the National School of Computer Science. We are grateful to all lab members for their technical advice and helpful discussions.

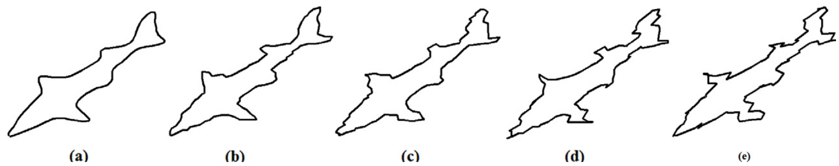

Fig. 18. An example of a contour with increasing Gaussian noise. (a) The original contour. σ from (b) to (e) increases from 0.2 to 0.8.

Appendix

The completeness's demonstration is taken from [78]. We denoted the parameterization of Γ by $C(s)$ and let the tangent vector is $t(s)$. The derivative of $t(s)$, denoted by $t_s(s)$, is given as follows:

$$t_s(s) = \kappa(s)(-t(s,y), t(s,x)) \tag{A.1}$$

Since $t(s)$ is a unit vector, we have now:

$$\begin{aligned} \frac{d(t(s,x)^2+t(s,y)^2)}{ds} &= 2t(s,x)t_s(s,x) + 2t(s,y)t_s(s,y) \\ &= 2 < (t(s,x), t(s,y)), (t_s(s,x), t_s(s,y)) > \\ &= 2 < (t(s,x), t(s,y)), \kappa(-t(s,y), t(s,x)) > \\ &= 0 \end{aligned} \tag{A.2}$$

It implies that $t_s(s) = \kappa(s).N(s)$ where $N(s)$ is the unit normal vector. The uniqueness of the solution of the differential equation of order 1 (A.1) implies that the respective tangent vectors $t^1(s)$ and $t^2(s)$ of two standard curvilinear parameterizations $C^1(s)$ and $C^2(s)$ having the same curvature functions κ are obtained from one another up to a planar displacement.

References

[1] David G. Kendall, Shape manifolds, procrustean metrics, and complex projective spaces, Bull. Lond. Math. Soc. 16 (2) (1984) 81–121.

[2] Eric Klassen, Anuj Srivastava, M. Mio, Shantanu H. Joshi, Analysis of planar shapes using geodesic paths on shape spaces, IEEE Trans. Pattern Anal. Mach. Intell. 26 (3) (2004) 372–383.

[3] Anuj Srivastava, Eric Klassen, Shantanu H. Joshi, Ian H. Jermyn, Shape analysis of elastic curves in euclidean spaces, IEEE Trans. Pattern Anal. Mach. Intell. 33 (7) (2011) 1415–1428.

[4] Shantanu H. Joshi, Jingyong Su, Zhengwu Zhang, Boulbaba Ben Amor, Elastic shape analysis of functions, curves and trajectories, Riemannian Comput. Comput. Vis. (2016) 211–231.

[5] Fatih Porikli, Oncel Tuzel, Peter Meer, Designing a boosted classifier on Riemannian manifolds, Riemannian Comput. Comput. Vis. (2016) 281–301.

[6] Jia Deng, Wei Dong, Richard Socher, Li-Jia Li, Kai Li, Li Fei-Fei, Imagenet: A large-scale hierarchical image database, 2009, pp. 248–255.

[7] Olga Russakovsky, Jia Deng, Hao Su, Jonathan Krause, Sanjeev Satheesh, Sean Ma, Zhiheng Huang, Andrej Karpathy, Aditya Khosla, Michael Bernstein, et al., Imagenet large scale visual recognition challenge, Int. J. Comput. Vis. 115 (3) (2015) 211–252.

[8] Mohammad Rastegari, Vicente Ordonez, Joseph Redmon, Ali Farhadi, Xnor-net: Imagenet classification using binary convolutional neural networks, in: European Conference on Computer Vision, Springer, 2016, pp. 525–542.

[9] Priya Goyal, Piotr Dollár, Ross Girshick, Pieter Noordhuis, Lukasz Wesolowski, Aapo Kyrola, Andrew Tulloch, Yangqing Jia, Kaiming He, Accurate, large minibatch sgd: Training imagenet in 1 h, 2017, arXiv preprint arXiv:1706.02677.

[10] Karen Simonyan, Andrew Zisserman, Very deep convolutional networks for large-scale image recognition, 2014, arXiv preprint arXiv:1409.1556.

[11] Alex Krizhevsky, Ilya Sutskever, Geoffrey E. Hinton, Imagenet classification with deep convolutional neural networks, 2012, pp. 1097–1105.

[12] Faouzi Ghorbel, Towards a unitary formulation for invariant image description: Application to image coding, Annals Telecommun. 53 (5) (1998) 242–260.

[13] Thomas R. Crimmins, A complete set of Fourier descriptors for two-dimensional shapes, IEEE Trans. Syst. Man Cybern. 12 (6) (1982) 848–855.

[14] Alireza Khotanzad, Hua Yaw Hong, Invariant image recognition by zernike moments, IEEE Trans. Pattern Anal. Mach. Intell. 12 (5) (1990) 489–497.

[15] Faouzi Ghorbel, Stephane Derrode, Rim Mezhoud, Tarek Bannour, Sami Dhahbi, Image reconstruction from a complete set of similarity invariants extracted from complex moments, Pattern Recognit. Lett. 27 (12) (2006) 1361–1369.

[16] Gösta H. Granlund, Fourier preprocessing for hand print character recognition, IEEE Trans. Comput. (2) (1972) 195–201.

[17] Ming-Kuei Hu, Visual pattern recognition by moment invariants, IRE Trans. Inf. Theory 8 (2) (1962) 179–187.

[18] Farzin Mokhtarian, Sadegh Abbasi, Josef Kittler, Robust and efficient shape indexing through curvature scale space, in: Proceedings of the 1996 British Machine and Vision Conference, BMVC, vol. 96, 1996.

[19] P.T. Yap, P. Raveendran, S.H. Ong, Chebyshev moments as a new set of moments for image reconstruction, in: Proceedings. IJCNN'01, in: International Joint Conference on Neural Network, vol. 4, 2001, pp. 2856–2860.

[20] X.Y. Jiang, Horst Bunke, Simple and fast computation of moments, Pattern Recognit. 24 (8) (1991) 801–806.

[21] Milan Sonka, Vaclav Hlavac, Roger boyle image processing, Anal. Mach. Vis. (1993) 10.

[22] Dengsheng Zhang, Image retrieval based on shape, Ph.D. Thesis, 2002.

[23] Whoi-Yul Kim, Yong-Sung Kim, A region-based shape descriptor using zernike moments, Signal Process., Image Commun. 16 (1) (2000) 95–102.

[24] G.Y. Yang, H.Z. Shu, Christine Toumoulin, Guo-Niu Han, Limin M. Luo, Efficient legendre moment computation for grey level images, Pattern Recognit. 39 (1) (2006) 74–80.

[25] Ch Rao, S. Srinivas Kumar, B. Chandra Mohan, et al., Content based image retrieval using exact legendre moments and support vector machine, 2010, arXiv preprint arXiv:1005.5437.

[26] Dengsheng Zhang, Guojun Lu, Generic Fourier descriptor for shape-based image retrieval, in: IEEE International Conference on Multimedia and Expo, vol. 1, 2002, pp. 425–428.

[27] Dengsheng Zhang, Guojun Lu, Enhanced generic Fourier descriptors for object-based image retrieval, in: IEEE International Conference on Acoustics, Speech, and Signal Processing, ICASSP, vol. 4, 2002, IV–3668.

[28] Cem Direkoglu, Mark S. Nixon, Shape classification using multiscale Fourier-based description in 2-D space, in: 9th International Conference on Signal Processing, 2008, pp. 820–823.

[29] Stephane Derrode, Faouzi Ghorbel, Robust and efficient Fourier–Mellin transform approximations for gray-level image reconstruction and complete invariant description, Comput. Vis. Image Underst. 83 (1) (2001) 57–78.

[30] Byung-Woo Hong, Emmanuel Prados, Stefano Soatto, Luminita Vese, Shape representation based on integral kernels: Application to image matching and segmentation, in: IEEE Computer Society Conference on Computer Vision and Pattern Recognition, vol. 1, 2006, pp. 833–840.

[31] Kaushik Chakrabarti, Michael Ortega-Binderberger, Kriengkrai Porkaew, Sharad Mehrotra, Similar shape retrieval in mars, in: IEEE International Conference on Multimedia and Expo, vol. 2, 2000, pp. 709–712.

[32] Harry Blum, A Transformation for Extracting Descriptors of Shape, MIT press, 1967.

[33] Thomas B. Sebastian, Philip N. Klein, Benjamin B. Kimia, Recognition of shapes by editing their shock graphs, IEEE Trans. Pattern Anal. Mach. Intell. 26 (5) (2004) 550–571.

[34] Kaleem Siddiqi, Benjamin B. Kimia, A shock grammar for recognition, in: IEEE Computer Society Conference on Computer Vision and Pattern Recognition, 1996, pp. 507–513.

[35] Krystian Mikolajczyk, Cordelia Schmid, Indexing based on scale invariant interest points, 1, 2001, pp. 525–531.

[36] David G. Lowe, Distinctive image features from scale-invariant keypoints, Int. J. Comput. Vis. 60 (2) (2004) 91–110.

[37] Svetlana Lazebnik, Cordelia Schmid, Jean Ponce, A sparse texture representation using local affine regions, IEEE Trans. Pattern Anal. Mach. Intell. 27 (8) (2005) 1265–1278.

[38] Anna Bosch, Andrew Zisserman, Xavier Muñoz, Scene classification via plsa, 2006, pp. 517–530.

[39] Herbert Bay, Tinne Tuytelaars, Luc Van Gool, Surf: Speeded up robust features, in: European Conference on Computer Vision, Springer, 2006, pp. 404–417.

[40] Herbert Bay, Andreas Ess, Tinne Tuytelaars, Luc Van Gool, Speeded-up robust features, SURF, Comput. Vis. Image Underst. 110 (3) (2008) 346–359.

[41] Eric Persoon, King-Sun Fu, Shape discrimination using Fourier descriptors, IEEE Trans. Pattern Anal. Mach. Intell. (3) (1986) 388–397.

[42] Timothy P. Wallace, Paul A. Wintz, An efficient three-dimensional aircraft recognition algorithm using normalized Fourier descriptors, Comput. Graph. Image Process. 13 (2) (1980) 99–126.

[43] Faouzi Ghorbel, Stability of invariant Fourier descriptors and its inference in the shape classification, in: Pattern Recognition, in: 11th IAPR International Conference on Image, Speech and Signal Analysis, 1992, pp. 130–133.

[44] Donald D. Hoffman, Whitman A. Richards, Parts of recognition, Cognition 18 (1) (1984) 65–96.

[45] Chengzhuan Yang, Qian Yu, Multiscale Fourier descriptor based on triangular features for shape retrieval, Signal Process., Image Commun. (2018).
[46] Naif Alajlan, Ibrahim El Rube, Mohamed S. Kamel, George Freeman, Shape retrieval using triangle-area representation and dynamic space warping, Pattern Recognit. 40 (7) (2007) 1911–1920.
[47] Foteini Fotopoulou, George Economou, Multivariate angle scale descriptor of shape retrieval, Proc. Signal. Process. Appl. Math. Electron. Commun. (2011) 105–108.
[48] Thomas B. Sebastian, Philip N. Klein, Benjamin B. Kimia, On aligning curves, IEEE Trans. Pattern Anal. Mach. Intell. 25 (1) (2003) 116–125.
[49] Serge Belongie, Jitendra Malik, Jan Puzicha, Shape matching and object recognition using shape contexts, IEEE Trans. Pattern Anal. Mach. Intell. 24 (4) (2002) 509–522.
[50] Haibin Ling, David W. Jacobs, Shape classification using the inner-distance, IEEE Trans. Pattern Anal. Mach. Intell. 29 (2) (2007) 286–299.
[51] Jun Xie, Pheng-Ann Heng, Mubarak Shah, Shape matching and modeling using skeletal context, Pattern Recognit. 41 (5) (2008) 1756–1767.
[52] Chunjing Xu, Jianzhuang Liu, Xiaoou Tang, 2D shape matching by contour flexibility, IEEE Trans. Pattern Anal. Mach. Intell. 31 (1) (2009) 180–186.
[53] Kaleem Siddiqi, Benjamin B. Kimia, Parts of visual form: Computational aspects, IEEE Trans. Pattern Anal. Mach. Intell. 17 (3) (1995) 239–251.
[54] Stefano Berretti, Alberto Del Bimbo, Pietro Pala, Retrieval by shape similarity with perceptual distance and effective indexing, IEEE Transactions Multimed. 2 (4) (2000) 225–239.
[55] Mohammad Reza Daliri, Vincent Torre, Classification of silhouettes using contour fragments, Comput. Vis. Image Underst. 113 (9) (2009) 1017–1025.
[56] Xin Shu, Xiao-Jun Wu, A novel contour descriptor for 2D shape matching and its application to image retrieval, Image Vis. Comput. 29 (4) (2011) 286–294.
[57] Glauco V. Pedrosa, Marcos A. Batista, Celia A.Z. Barcelos, Image feature descriptor based on shape salience points, Neurocomputing 120 (2013) 156–163.
[58] Nacera Laiche, Slimane Larabi, Farouk Ladraa, Abdelnour Khadraoui, Curve normalization for shape retrieval, Signal Process., Image Commun. 29 (4) (2014) 556–571.
[59] Hassan Silkan, S.E. Ouatik, Abdelmounim Lachkar, Mohammed Meknassi, A novel shape descriptor based on extreme curvature scale space map approach for efficient shape similarity retrieval, in: Fifth International Conference on Signal-Image Technology and Internet-Based Systems, SITIS, 2009, pp. 160–163.
[60] Tomasz Adamek, Noel E. O'Connor, A multiscale representation method for nonrigid shapes with a single closed contour, IEEE Trans. Circuits Syst. Video Technol. 14 (5) (2004) 742–753.
[61] Ameni Benkhlifa, Faouzi Ghorbel, A novel 2D contour description generalized curvature scale space, in: International Workshop on Representations, Analysis and Recognition of Shape and Motion From Imaging Data, 2016, pp. 129–140.
[62] David Sankoff, Joseph B. Kruskal, in: David Sankoff, Joseph B. Kruskal (Eds.), Time Warps, String Edits, and Macromolecules: The Theory and Practice of Sequence Comparison, Reading: Addison-Wesley Publication, 1983.
[63] Chotirat Ann Ratanamahatana, Eamonn Keogh, Everything you know about dynamic time warping is wrong, in: Third Workshop on Mining Temporal and Sequential Data, 2004, pp. 22–25.
[64] Ninad Thakoor, Jean Gao, Sungyong Jung, Hidden Markov model-based weighted likelihood discriminant for 2-D shape classification, IEEE Trans. Image Process. 16 (11) (2007) 2707–2719.
[65] Manuele Bicego, Vittorio Murino, Mario A.T. Figueiredo, Similarity-based classification of sequences using hidden Markov models, Pattern Recognit. 37 (12) (2004) 2281–2291.
[66] Longin Jan Latecki, Rolf Lakamper, T. Eckhardt, Shape descriptors for non-rigid shapes with a single closed contour, in: IEEE Conference on Computer Vision and Pattern Recognition, vol. 1, 2000, pp. 424–429.
[67] Oskar Söderkvist, Computer vision classification of leaves from swedish trees, 2001.
[68] Bastian Leibe, Bernt Schiele, Analyzing appearance and contour based methods for object categorization, in: IEEE Computer Society Conference on Computer Vision and Pattern Recognition, vol. 2, 2003, II–409.
[69] Longin Jan Latecki, Rolf Lakamper, Shape similarity measure based on correspondence of visual parts, IEEE Trans. Pattern Anal. Mach. Intell. 22 (10) (2000) 1185–1190.
[70] Smit Marvaniya, Raj Gupta, Anurag Mittal, Adaptive locally affine-invariant shape matching, Mach. Vis. Appl. 29 (4) (2018) 553–572.
[71] Junwei Wang, Xiang Bai, Xinge You, Wenyu Liu, Longin Jan Latecki, Shape matching and classification using height functions, Pattern Recognit. Lett. 33 (2) (2012) 134–143.
[72] Xiang Bai, Cong Rao, Xinggang Wang, Shape vocabulary: A robust and efficient shape representation for shape matching, IEEE Trans. Image Process. 23 (9) (2014) 3935–3949.
[73] Dengsheng Zhang, Guojun Lu, Study and evaluation of different Fourier methods for image retrieval, Image Vis. Comput. 23 (1) (2005) 33–49.
[74] Pedro F. Felzenszwalb, Joshua D. Schwartz, Hierarchical matching of deformable shapes, 2007, pp. 1–8.
[75] Yasser Ebrahim, Maher Ahmed, Wegdan Abdelsalam, Siu-Cheung Chau, Shape representation and description using the Hilbert curve, Pattern Recognit. Lett. 30 (4) (2009) 348–358.
[76] Nadia Payet, Sinisa Todorovic, Matching hierarchies of deformable shapes, in: GbRPR, 2009, pp. 1–10.
[77] Andrew Temlyakov, Brent C. Munsell, Jarrell W. Waggoner, Song Wang, Two perceptually motivated strategies for shape classification, in: IEEE Conference on Computer Vision and Pattern Recognition, CVPR, 2010, pp. 2289–2296.
[78] Gayatri Chakravorty Spivak, A Critique of Postcolonial Reason, Harvard university press, 1999.